



Photocatalytic properties of TiO₂ nanostructures of different morphology modified with various modifiers

Reinis Drunka^{*}, Janis Grabis, Dzidra Jankovica, Dzintra-Arija Rasmane, and Aija Krumina

Institute of Inorganic Chemistry, Riga Technical University, Paula Valdena St. 7, LV-1048, Riga, Latvia

Received 20 December 2018, accepted 13 March 2019, available online 23 April 2019

© 2019 Authors. This is an Open Access article distributed under the terms and conditions of the Creative Commons Attribution-NonCommercial 4.0 International License (<http://creativecommons.org/licenses/by-nc/4.0/>).

Abstract. Synthesis of TiO₂ nanotube coatings, nanoporous coatings, and nanofibres by using titanium anodizing, microplasma electrolytic oxidation, and microwave-assisted hydrothermal synthesis in different regimes was studied. Optimal conditions for each of the methods for obtaining nanostructures were determined. The obtained TiO₂ nanofibres and nanotube and nanoporous coatings were modified with Au, Ag, Pt, Pd, S, WO₃, and Eu₂O₃, nanoparticles to improve photocatalytic activity under ultraviolet and visible light irradiation. Photocatalytic properties of photocatalysts were tested by the degradation of methylene blue solution under the influence of ultraviolet and visible light irradiation. The obtained modified photocatalysts exhibited higher photocatalytic activity than pure TiO₂ nanostructured photocatalysts. Properties of modified photocatalysts obtained with different methods are compared.

Key words: photocatalysis, TiO₂, nanofibres, coatings, nanopores, nanotubes.

1. INTRODUCTION

In recent decades, much research has been focused on the properties of materials with a very small particle size [1]. Since the 1970s, TiO₂ has become one of the most widely studied photocatalysts in the world. It exhibits very high photocatalytic activity under ultraviolet (UV) irradiation, but still this photocatalytic activity is inadequate in visible (VIS) light [2,3]. It is necessary to reduce the width of the band gap (for pure TiO₂ anatase ~3.2 eV). This can be done by introducing a small amount of atoms or molecules of other elements into a TiO₂ anatase crystalline in place of oxygen vacancies [4]. Solar cells made from various modified TiO₂ nanostructures have shown that efficiency increased from 7% in 1991 to 12–13% at present, and with the use of such materials in direct sunlight their efficiency is

almost 2 times higher than in the VIS light because solar radiation also includes the spectral part of UV irradiation [5,6]. The efficiency of photocatalysts can also be improved by increasing the specific surface, which can be successfully realized by forming TiO₂ photocatalysts with different nanostructured surface morphology such as nanotube and nanoporous coatings or nanofibres [7–9].

Plasma electrolytic oxidation is an electrochemical method for the formation of oxide layers on metals such as Al, Ti, and Mg under electric microarc discharges. The method allows protective porous coatings and catalytically active layers of oxides to be formed [10–14].

The microwave-assisted hydrothermal method has unique advantages of uniform and rapid heating in comparison with the conventional methods. In addition, this method can significantly reduce the reaction time, leading to a fast crystallization and simplification of the preparation procedure [15].

^{*} Corresponding author, reinis.drunka@rtu.lv

Modified TiO₂ is able to degrade harmful organic compounds into less harmful ones; therefore, it has a wide range of possibilities for use in industrial plants as well as in wastewater treatment systems [16,17].

Previous studies have described many different methods for obtaining modified TiO₂ nanopowders. However, the practical use of such materials is complicated due to the problematic removal of the photocatalyst nanoparticles from the treated solution. Practical applications are surfacemounted TiO₂ photocatalysts. Prospective methods to achieve the aims of the research are anodization, microplasma electrolytic oxidation, and microwave-assisted synthesis combined with the modification of the chemical composition of the photocatalysts. The modification of TiO₂ with Au, Pt, Pd, Ag, WO₃, S, and Eu₂O₃ nanoparticles [18–24] is effective in increasing photocatalytic activity; however, the activity also depends on the modifier content, TiO₂ morphology, and particle size [25].

The aim of this research was to find out the best methods and conditions for the preparation of modified visible light active nanostructured TiO₂ photocatalysts and to compare properties of the obtained photocatalysts.

2. EXPERIMENTAL

2.1. Preparation of TiO₂ nanotubes

Coating of self-organized TiO₂ nanotube layers was prepared by electrochemical anodization of titanium foil in 200 mL of 0.2 M (NH₄)₂SO₄ electrolyte with 1 wt% hydrofluoric acid (HF) for 5–120 min at 20 V DC. A Teflon reaction vessel was used for this process. Platinum foil was used as the counter electrode.

2.2. Preparation of nanoporous TiO₂ coating

The coating of self-organized TiO₂ nanopore layers was prepared by using plasma electrolytic oxidation (PEO) of titanium dioxide foil in 0.5 M H₂SO₄ electrolyte with Pt foil used as the counter electrode. The current was 100–200 V DC and the experimental process was 3 min long.

2.3. Preparation of TiO₂ nanofibres

Three grams of TiO₂ anatase nanopowder (Sigma-Aldrich, ≥99.7%, <25 nm particle size) was dissolved in 670 mL of 10 M KOH at room temperature. This aqueous solution was poured into a microwave vessel made of Teflon. The microwave treatment was performed at 180–245 °C for 60 min by using an Anton Paar Master-wave BTR microwave system. The solution was stirred

with a speed of 700 rpm during the reaction time. The obtained solution was then cooled to room temperature and the TiO₂ particles were left to precipitate. After this procedure, the KOH solution was decanted from the vessel, and the obtained TiO₂ suspension was diluted with a large amount of deionized water to decrease the concentration of KOH.

Washing and decanting procedures were repeated several times. Finally, a certain amount 1 M HCl was added to the TiO₂ suspension to reduce its pH to 7.0. The obtained solution was filtered by using a 1.0-μm cellulose nitrate membrane filter. Particles were washed on the filter several times with deionized water and 96% ethanol. The powder was dried at 110 °C for 24 h. After drying, the TiO₂ nanofibre powder was stirred in 1 M HCl solution for 24 h to remove titanates. This procedure also allowed us to decrease the absorption of methylene blue (MB) on TiO₂ nanofibres surface.

2.4. Modification of TiO₂ nanostructures

The obtained TiO₂ nanostructures were modified with Au, Pt, Ag, Pd, and Eu₂O₃ nanoparticles by using the chemical precipitation method. The concentration of the modifier in the sample was about 1 wt%.

For the modification of the TiO₂ nanofibre sample with precious metals nanoparticles, 1.0 g of nanofibres was dispersed in 50 mL of an ethyl alcohol solution in an ultrasonic bath for 1 h. Then 50 mL of water was added to the suspension. The suspension was heated and stirred at 50 °C for 20 min. Then the pH was adjusted to 1–2 with diluted HCl (1 : 5).

Chloride solutions containing the modifier metal (Au, Pd) were prepared. The platinum-containing solution was obtained from H₂PtCl₆·6H₂O by dissolving it in water. The silver ion-containing solution was prepared from AgNO₃. The modifier concentration was controlled by adding a certain amount of water.

Solutions containing Au, Ag, Pt, and Pd were added to 0.18 M K₂CO₃ solution. The diluted ammonia solution was used to adjust the pH to 6.5–7. The resulting solutions were added to the TiO₂ nanofibre suspensions. The obtained solutions were stirred for 1 h and then small portions of H₄BNA were added. The solutions were filtered and the resulting samples were dried for 24 h at 120 °C.

Nanoporous and nanotube coating samples were modified with nanoparticles of precious metals by using the method of immersion into solutions containing the modifier. As the reducing agent, H₄BNA was used.

The nanotube coatings were doped with tungsten oxide by the anodization of TiO₂ foil mechanically rubbed with tungsten particles or by additional cathodic electrochemical deposition of the as-prepared TiO₂ nano-

tubes in 0.001 M peroxitungstic acid electrolyte for 5 min at 10 V DC.

For the modification of the nanoporous coating with Eu_2O_3 nanoparticles the method of cathodic electrochemical deposition in 0.001 M $\text{Eu}(\text{NO}_3)_3$ solution at 10 V DC for 5 min was used. For the nanofibre sample the chemical deposition method in 0.001 M $\text{Eu}(\text{NO}_3)_3$ solution and H_4BNA as the reducing agent was applied.

For sample modification with S, the calcination method in the H_2S gas flow at 380 °C for 2 h was used.

Samples were crystallized by calcination:

- Au, Pt, Ag, WO_3 , and Eu_2O_3 modified samples at 500 °C for 2 h;
- Pd modified sample at 120 °C for 2 h;
- S modified sample at 380 °C for 2 h.

2.5. Determination of photocatalytic activity

Photocatalytic properties of the obtained TiO_2 nanostructures were tested by using degradation of the MB solution under UV and VIS light irradiation. A FEK–56, 120 W mercury high-pressure UV lamp was used as the UV light source and a Philips Tornado 23 W halogen lamp as the VIS light source. The degradation process of the MB solution was controlled by a spectrophotometer (Jenway 6300). The absorption of the MB solution was measured at a wavelength of 664 nm. For the degradation of 100 mL of MB 0.1000 g of TiO_2 nanofibre powder and 1 cm² of nanopore or nanotube coating (7.2 mg/L) were used.

2.6. Analysis of physical properties

The morphology and oxide layer thickness were analysed with a scanning electron microscope system (Tescan Lyra) and a transmission electron microscope (FEI Tecnai). The specific surface area was obtained with the Brunauer–Emmett–Teller (BET) method and HROM 3 gas analyser.

An X-ray diffractometer Bruker AXS D8 Advance was used for phase content analysis of the obtained samples. The Scherrer equation was used for the calculation of the average crystallite size from XRD patterns.

The chemical content of the samples was analysed by a Bruker AXS Pioneer S4 X-ray fluorescence (XRF) spectrometer.

3. RESULTS

3.1. Properties of the obtained TiO_2 nanotube coatings

Regardless of the duration of anodization, all anodically prepared samples were found to have nanoparticle

coatings on their surface. The as-prepared TiO_2 nanotubes were X-ray amorphous, but after calcination at 500 °C for 2 h anatase nanotubes were obtained. The average diameter of the nanotubes was approximately equal in all cases, ranging from 76 to 85 nm. The optimum nanotube synthesis time was 30–45 min. In case titanium was anodized for a longer time, a dense titanium dioxide coating that overlapped TiO_2 nanotubes was noticed (Fig. 1). The results of the influence of anodizing time on the quality of TiO_2 nanotube coatings are summarized in Table 1.

After 60 min of anodizing, the nanotube layer was partly covered with a homogeneous TiO_2 layer, but after 120 min almost the whole nanotube layer was covered with it. Thus, such a model is not suitable for further research on photocatalysis. As the anodization time

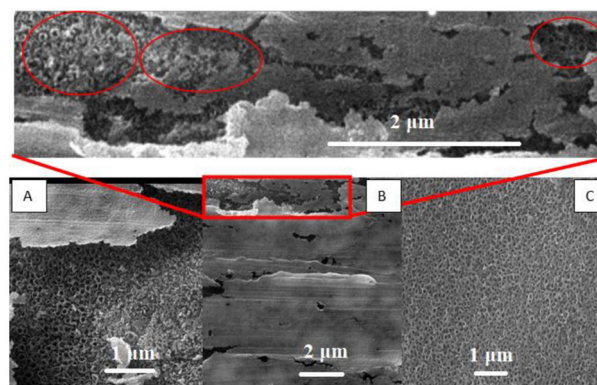


Fig. 1. Effect of time on the anodizing process and the formation of TiO_2 nanotube coating. A – TiO_2 nanotube coatings are covered by a dense TiO_2 layer; anodizing time 60 min. B – Nanotube coatings are practically covered everywhere by a dense TiO_2 layer, nanotubes are only visible in some places; anodizing time 120 min. C – TiO_2 nanotube coatings without defects; anodizing time 45 min.

Table 1. Influence of anodizing time on the formation of nanotube coating. The box highlights the best results

Time, min	Nanotubes were obtained	Surface defects	Thickness of TiO_2 coating, μm
5	Yes	Yes	5.3
10	Yes	Yes	7.2
15	Yes	Yes	9.7
30	Yes	No	12.2
45	Yes	No	16.4
60	Yes	Nanotubes covered with oxide layer	22.0
120	Yes	Nanotubes covered with oxide layer	33.5

lengthened, the thickness of the TiO₂ layer increased from 5.3 to 33.5 μm.

3.2. Properties of the obtained TiO₂ nanoporous coatings

It was established that the resulting TiO₂ nanoporous coating contained both crystalline anatase and rutile phases. Rutile specific maxima were observed at 27.5, 36, 42, and 52.3 2θ degrees (Fig. 2). Also after calcination at 500 °C for 2 h the TiO₂ nanoporous coating on titanium foil contained anatase and rutile crystalline phases. The formation of the rutile phase is associated with the temperature rise in the microspark discharges.

The average crystallite size of the TiO₂ nanoporous coatings was 40 nm for anatase and 50 nm for rutile. The relatively high average crystallite size indicates a strong temperature effect on the surface of the sample during synthesis. The SEM micrograph (Fig. 3) shows that the surface of the titanium foil has a porous coating. Most of the pores are in the range of 100–350 nm, but smaller pores with a diameter of 30–70 nm are also visible. The surface of the titanium foil is homogeneously coated with a layer of porous oxide. The thickness of the TiO₂ layer was determined to be in the range of 38–127 μm (Table 2). Separate samples started to dissolve during the PEO process, also some crystalline particles were deposited on the surface of the obtained porous coating and other surface defects were noticed.

The current decreased during the experiment significantly. When a voltage of 160 V was selected, the current reached 8 A at the beginning of the experiment, but after 3 min it was only 0.2 A. This change in the

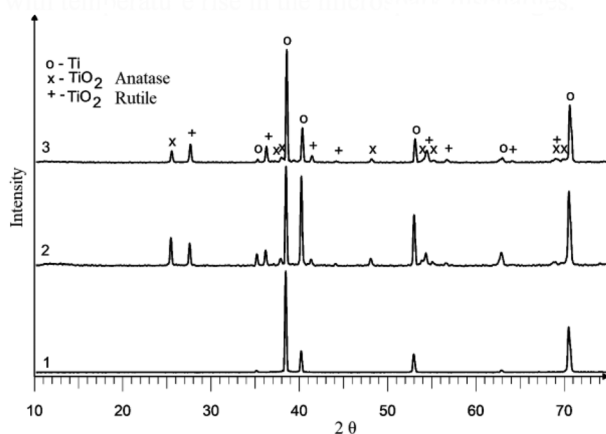


Fig. 2. XRD curves of nanoporous TiO₂ samples obtained with the PEO method: 1 – titanium plate before processing; 2 – titanium foil coated with a TiO₂ nanoporous coating; 3 – titanium foil coated with a TiO₂ nanoporous coating, calcinated at 500 °C for 2 h.

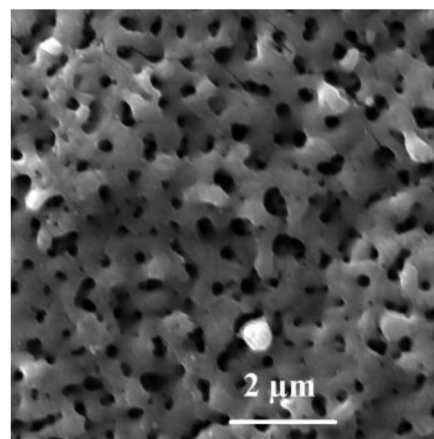


Fig. 3. Micrograph of TiO₂ nanoporous coating obtained with the PEO method.

Table 2. Influence of PEO parameters on the formation of porous coating. The box highlights the best results

Voltage, V	Nano-porous coating	Defects of surface	Thick-ness of coating, μm	Average diameter of nano-pores, nm
100	No	Yes	45	–
140	Yes	Yes	54	93
160	Yes	No	71	135
180	Yes	The edges of foil slightly soluble	62	183
200	Yes	The edges of foil rapidly dissolved	58	192

current is due to the rapid increase in the thickness of the TiO₂ layer on the titanium surface, which greatly increases its resistance.

3.3. Properties of the obtained TiO₂ nanofibres

With a synthesis pressure of over 19.3 bar the formation of thin-film coatings on the reactor cylinder walls was observed. The coating showed individual sets of fibres whose orientation coincided with the direction of the mixing of the reaction solution. The coating was dense but not mechanically durable. Figure 4 shows the obtained TiO₂ nanofibre coating after its removal from the microwave synthesis reactor wall. It was determined that with increasing reaction temperature and pressure the morphology of TiO₂ nanofibres improved (Table 3). When the reaction temperature and pressure were

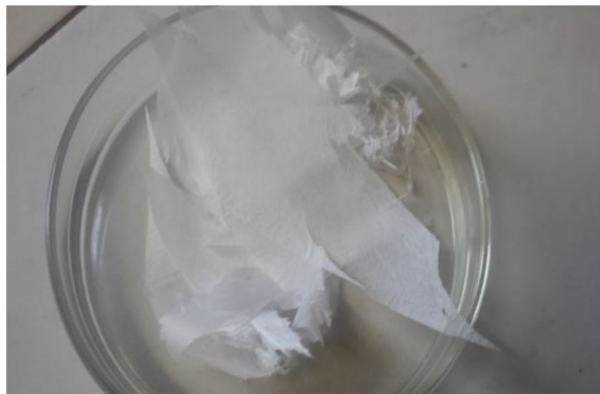


Fig. 4. TiO₂ nanofibre coating obtained with the microwave synthesis method placed on a Petri plate (Petri plate diameter 90 mm).

Table 3. Influence of temperature and pressure on TiO₂ nanofibre properties. The box highlights the best results

Temperature, °C	Pressure, bar	TiO ₂ morphology after synthesis	Specific surface, m ² /g
180	5.1	Nanocrystalline agglomerates	21.8
200	9.6	Nanocrystalline agglomerates, small amount of nanofibres	42.0
210	12.2	Mixture of nanocrystallite agglomerates and nanofibres	67.4
220	15.4	Nanofibres	98.7
230	21.9	Nanofibres	129.0
240	27.3	Nanofibres	151.9
245	29.1	Nanofibres	158.5

raised, the specific surface of TiO₂ nanofibres increased. The optimum temperature and pressure for nanofibre synthesis were 240–245 °C and 27.3 to 29.1 bar. Under these conditions the specific surface reached 151.9 to 158.5 m²/g.

Figure 5 shows TEM micrographs with different magnifications of TiO₂ nanofibres. When the synthesis temperature was increased to 240 °C, the pressure reached 27.3 bar and the fibres obtained on the reactor walls had a certain orientation. The direction of the fibre filament coincided in most fibres with that of mixing the solution. An increase in the synthesis temperature up to 245 °C led to an improvement in the orderliness of TiO₂ nanofibres orientation. Figure 6 shows SEM micrographs of TiO₂ nanofibres. Fibres obtained on the reactor walls are arranged in correspondence of the solution mixing

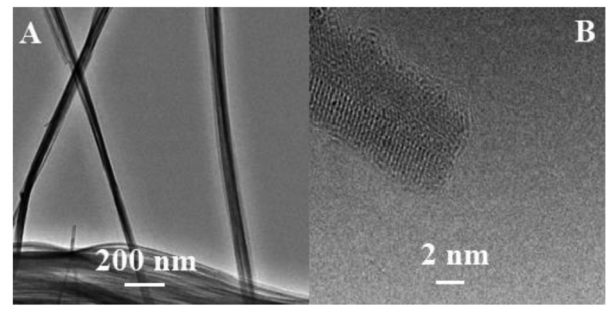


Fig. 5. TEM micrographs of TiO₂ nanofibres at different magnifications.

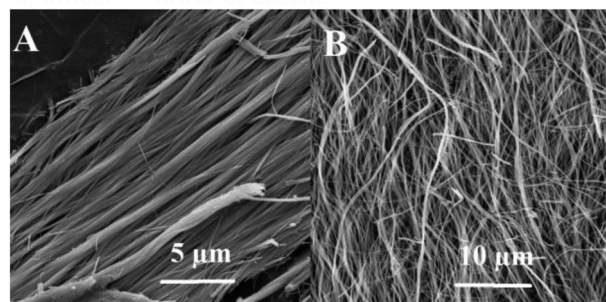


Fig. 6. SEM micrographs at different magnifications of TiO₂ nanofibres obtained with microwave synthesis method from the reactor walls at different reaction conditions.

direction. The orientation of the fibres obtained from the suspension is not specified.

No impurities of raw material residues were observed in nanofibre morphology. The individual nanofibres could reach a length of 500 μm. After calcination at 500 °C for 2 h TiO₂ nanofibre samples were characterized by anatase maxima but there were no rutile-specific maxima even if the TiO₂ P25 anatase–rutile nanopowders mixture was used as the raw material for nanofibre microwave synthesis. The samples also showed the presence of various potassium titanates as well as TiO₂ monocline. After TiO₂ nanofibre samples were treated in diluted hydrochloric acid for 12 h, the presence of potassium titanate was significantly lower or absent.

TiO₂ nanofibres also exhibited the formation of a monoclinic TiO₂ phase (Fig. 7). In addition, the characteristic maxima of this phase overlapped with K₂Ti₁₃O₆ maxima; therefore, after processing the samples in hydrochloric acid for 12 h and calcination at 500 °C for 2 h the X-ray diffraction patterns of the samples showed intensive maxima in the group intervals of 28.0–35.0, 41.5–45.5, and 55.75–61.5 2 θ degrees. The TiO₂ monoclinic phase content of the samples increased with the increasing temperature and pressure in the reaction vessel. At altering the reaction conditions no other

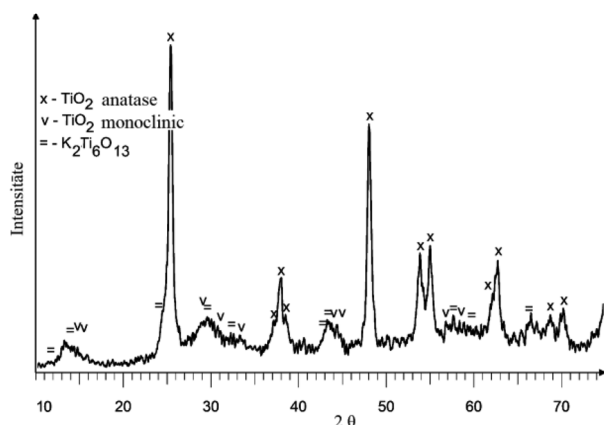


Fig. 7. XRD pattern of TiO₂ nanofibres prepared with the microwave-assisted synthesis method (before washing in hydrochloric acid).

changes in the phase composition were observed. Calcination at 500 °C did not affect the size and shape of the obtained nanofibres.

3.4. Properties of modified TiO₂ nanostructures

Figure 8 shows SEM micrographs of modified TiO₂ photocatalysts morphology. The gold content in these samples was about 1%. In order to highlight the modifier particles it is generally recommended that a backscattered electrons (BSE) detector should be used to obtain SEM micrographs.

TEM micrographs at various magnifications of TiO₂ nanofibres modified with 1% Au are shown in Fig. 9. It was determined that the average crystallite sizes of modifiers ranged from 10 to 30 nm depending on the modifier and the method of preparation. The various properties of modified TiO₂ nanofibres and raw materials are summarized in Table 4. It shows that compared to the raw material the specific surface area of the obtained

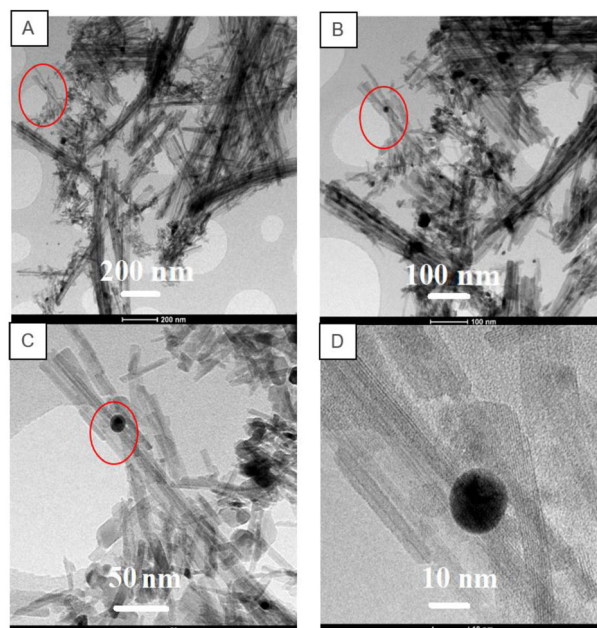


Fig. 9. TEM microphotographs of TiO₂ nanofibres modified with 1% Au at different magnifications.

nanofibres was considerably larger, ranging from 58.7 to 83.7 m²/g, and the crystallite size of the modifier was in the range 10–30 nm.

The photocatalytic properties of various modified TiO₂ nanostructures under UV and VIS illumination are summarized in Figs 10–15. It was noticed that the photocatalytic activity under UV irradiation was very similar for all samples modified with precious metals but a wider distribution of results was observed in the case of VIS irradiation.

The results of the study of the photocatalytic activity of various modified TiO₂ nanofibres are shown in Fig. 10. It can be seen that all modified samples exhibit at least 28% higher activity than the pure TiO₂ nanofibre

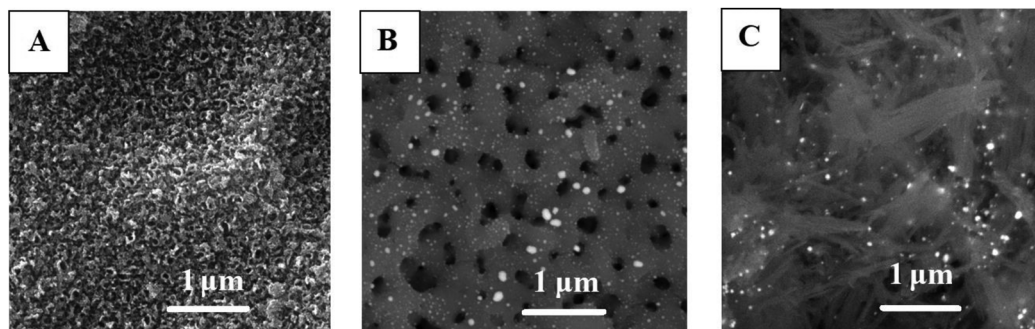
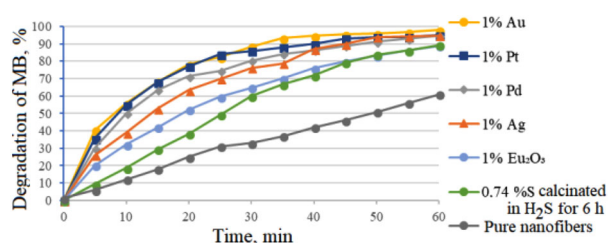


Fig. 8. SEM micrographs of the morphology of TiO₂ modified with 1% Au: A – nanotube coating; B – nanoporous coating; C – nanofibres. A BSE detector was used to obtain images B and C.

Table 4. Summary of properties

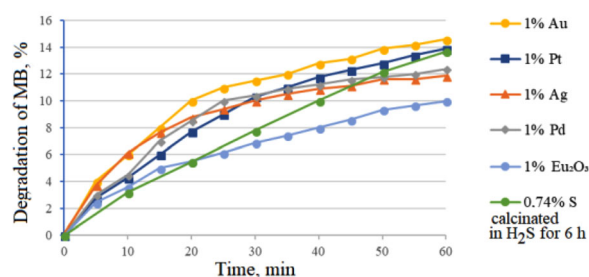
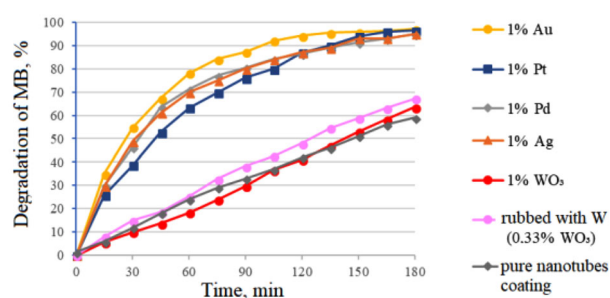
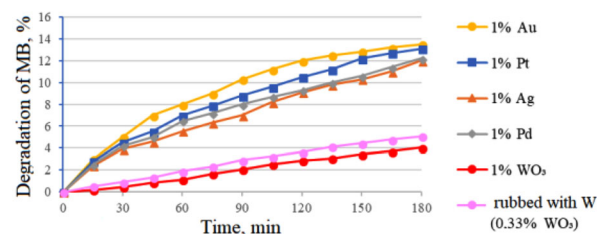
Sample ^a	Content of modifier, % (XRF)	Specific surface, m ² /g (BET)
TiO ₂ -NF-1%-Au	0.95	73.1
TiO ₂ -NF-1%-Pt	1.10	75.2
TiO ₂ -NF-1%-Pd	1.10	74.1
TiO ₂ -NF-1%-Ag	1.12	74.7
TiO ₂ -NF-6h-H ₂ S	0.74	78.8
TiO ₂ -NF-1%-Eu ₂ O ₃	1.03	58.7
TiO ₂ nanofibres	–	158.5
TiO ₂ nanofibres after calcination at 500 °C for 2 h	–	85.4
TiO ₂ anatase nanopowder	–	43.5

^a NF in the sample code stands for nanofibre.

**Fig. 10.** Photocatalytic activity of modified TiO₂ nanofibres under UV irradiation.

sample. The degradation of MB reached 89.20–98.03% per hour. Under UV irradiation the non-metallic modifiers exhibited lower photocatalytic activity than the precious metal modifiers. The result of the sulphur-modified sample with a sulphur content of only 0.77% under VIS illumination (Fig. 11) stands out as capable of degrading up to 13.70% of the MB per hour, which is only 0.9% less than the highest result shown by the TiO₂ nanofibres sample modified with 1% Au.

Photocatalytic properties under UV and VIS irradiation of TiO₂ nanotubes modified with various dopants are summarized in Figs 12 and 13. It can be seen that precious metals significantly improved the properties of photocatalysts compared to the WO₃ modifier. Although WO₃ itself is an active photocatalyst, its photocatalytic activity under UV irradiation did not improve significantly when combined with TiO₂. It was ascertained that when both methods were used to modify samples with WO₃ nanoparticles, the obtained samples showed low photocatalytic activity under UV and VIS irradiation. Under UV exposure the photocatalytic activity was almost identical to that of non-modified TiO₂ nanotubes. It was observed that the photocatalytic activity of precious

**Fig. 11.** Photocatalytic activity of modified TiO₂ nanofibres under VIS illumination.**Fig. 12.** Photocatalytic activity of modified TiO₂ nanotube coatings under UV irradiation.**Fig. 13.** Photocatalytic activity of modified TiO₂ nanotube coatings under VIS illumination.

metals-modified TiO₂ nanotube coatings and that of TiO₂ nanofibres modified with gold nanoparticles under UV irradiation were very similar, and therefore it is appropriate to use the cheapest modifier – silver, which degraded only a 2.01% lower amount of MB in 3 h compared to 1% Au-modified TiO₂ nanotubes coating photocatalyst. Under VIS illumination the most active sample with a 1% Au content degraded 13.10% of the MB in 3 h, while the 1% WO₃-modified sample showed the least favourable result, degrading only 4.03% of the MB. Comparison of the photocatalytic activity of the 1% Au-modified TiO₂ nanotubes coating with a modified TiO₂ nanofibres sample containing 1% Au revealed that their results differed only by 1.50%. However, it should be taken into account that it took the modified nanotubes

sample to reach such a result a 3 times longer period of time. The amount of MB degraded by 1% silver-modified TiO₂ nanotube coating differed by 1.50% from the photocatalyst with a 1% Au content; so it is also economically more profitable to manufacture industrial catalysts modified with silver. The chosen modifiers increased the modified TiO₂ nanotube coatings activity in the following order: WO₃ << Ag < Pd < Pt < Au.

As the method of producing nanotube coatings was the same in all cases, it can be concluded that the activity of modified TiO₂ nanotube photocatalysts was influenced only by the content of the modifier, the modification method, and particle size. With the increasing content of the modifier in the sample, also its crystallite size increased slightly.

Comparison of TiO₂ nanoporous samples with a 1% modifier content showed that they had 20.9–45.9% higher activity under UV irradiation than pure TiO₂ nanoporous samples. The photocatalytic activity of samples modified with different precious metals was practically the same (Fig. 14). Therefore, it is the most expeditious to use as the modifier the cheapest of them – silver.

Although during the first hour the TiO₂ nanoporous coating sample modified with 1% S showed practically the same activity as the unmodified sample, subsequent measurements indicated that the amount of the degraded MB rapidly increased, reaching 74.0% in 3 h. A sample modified with 1% Eu₂O₃ degraded 85.12% of the MB under UV irradiation and 9.67% under VIS irradiation in a 3-h experiment (Fig. 15). A TiO₂ nanoporous coating sample modified with 1% Ag was also shown to be active. It degraded 94.76% of the MB in 3 h. As silver is cheaper than gold, it is economically advantageous to use silver also in this case because the effect compared to the catalyst containing 1% gold was almost the same. The best result under VIS illumination was shown by a sample of TiO₂ nanoporous coating modified with gold nanoparticles. The activity of modified TiO₂ nanoporous coatings photocatalysts increased in the following order: S < Eu₂O₃ < Ag < Pd < Pt < Au. The worst result was shown by sulphur: the modified sample was able to degrade only 7.78% of the MB within 3 h under VIS illumination.

The modified TiO₂ nanoporous coating samples showed lower photocatalytic activity than similarly modified TiO₂ nanofibres and nanotubes coatings due to the fact that these samples had a smaller specific surface. Possibly, the presence of rutile in the TiO₂ coating enables to improve the photocatalytic activity of the photocatalyst obtained similarly to the standard P25 material widely used as a reference material for studies of photocatalysis.

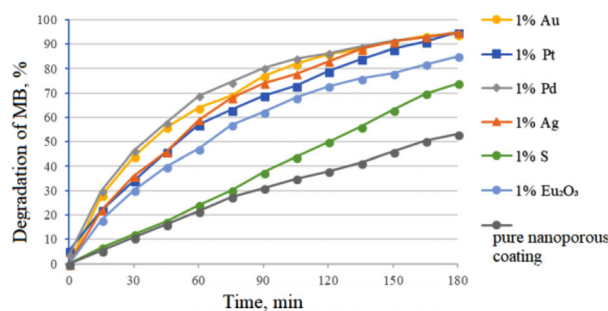


Fig. 14. Photocatalytic activity of modified TiO₂ nanoporous coatings under UV irradiation.

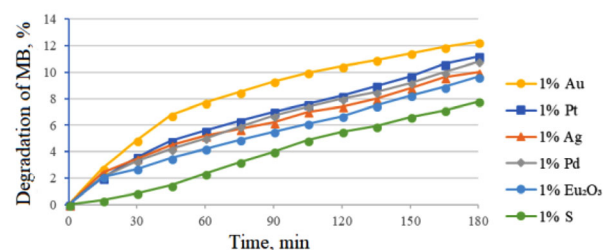


Fig. 15. Photocatalytic activity of modified TiO₂ nanoporous coatings under VIS illumination.

Comparison of the measurement results of the photocatalytic activity of the obtained modified nanoporous coatings with similarly modified TiO₂ nanotube coatings and TiO₂ nanofibres samples indicated that gold-modified samples showed the best results with a degradation rate from 94.86% to 98.03% of the MB. The modified nanofibre samples reached the same result 3 times faster than the modified nanotube and nanoporous coating samples. A 1% gold-modified TiO₂ nanotube coating sample showed only a 2.15% higher result in 3 h than a TiO₂ nanoporous coating photocatalyst with a similar gold content.

4. CONCLUSIONS

Depending on the type of nanostructure the amount of the degraded MB with the same modifier content increased in the following order: nanoporous coatings < nanotube coatings < nanofibres. Moreover, 0.1 g of modified TiO₂ nanofibres was capable of degrading the same amount of MB per hour as similarly modified TiO₂ nanotube coatings or TiO₂ nanoporous coatings with a surface area of 1 cm² in 3 h under both UV and VIS irradiation. Modification with gold nanoparticles increased the photocatalytic activity of all obtained TiO₂ nanostructures most of all. The use of surface-fixed modified TiO₂ photocatalysts in practice is more convenient and

cheaper compared to powder-type photocatalysts. It is possible to optimize the cost of the production of catalysts by reducing the content of precious metals in the photocatalyst or replacing it with the cheapest of precious metals, such as silver. This would not significantly change the photocatalytic activity of the photocatalyst.

ACKNOWLEDGEMENTS

This work was supported by the European Regional Development Fund within the project I.1.1.1/16/A/079 ‘Development of active under sunlight immobilized TiO₂-ZnO fixed photocatalysts’. The publication costs of this article were covered by the Estonian Academy of Sciences.

REFERENCES

- Dolez, P. I. Nanomaterials definitions, classifications, and applications. In *Nanoengineering*. Elsevier, 2015, 3–40.
- Fujishima, A. and Honda, K. Electrochemical photolysis of water at a semiconductor electrode. *Nature*, 1972, **238**, 37–38.
- Fujishima, A., Rao, T. N., and Tryk, D. A. Titanium dioxide photocatalysis. *J. Photochem. Photobiol. C Photochem. Rev.*, 2000, **1**, 1–21.
- Cao, Z., Zhu, S., Qu, H., Qi, D., Ziener, U., Yang, L., et al. Preparation of visible-light nano-photocatalysts through decoration of TiO₂ by silver nanoparticles in inverse miniemulsions. *J. Colloid Interface Sci.*, 2014, **435**, 51–58.
- Xiao, J., Tao, R., Costa, B. F. O., and Paixão, J. A. Nanostructured titania photoanodes for dye solar cells. *Mater. Today Proc.*, 2015, **2**, 141–146.
- Grätzel, M. The artificial leaf, molecular photovoltaics achieve efficient generation of electricity from sunlight. *Coord. Chem. Rev.*, 1991, **111**, 167–174.
- Song, H., Shang, J., and Suo, C. Fabrication of TiO₂ nanotube arrays by rectified alternating current anodization. *J. Mater. Sci. Technol.*, 2015, **31**, 23–29.
- Bayati, M. R., Moshfegh, A. Z., and Golestani-Fard, F. On the photocatalytic activity of the sulfur doped titania nano-porous films derived via micro-arc oxidation. *Appl. Catal. Gen.*, 2010, **389**, 60–67.
- Liu, Y., Yu, H., Lv, Z., Zhan, S., Yang, J., Peng, X., et al. Simulated-sunlight-activated photocatalysis of Methylene Blue using cerium-doped SiO₂/TiO₂ nanostructured fibers. *J. Environ. Sci.*, 2012, **24**, 1867–1875.
- Espino-Estévez, M. R., Fernández-Rodríguez, C., González-Díaz, O. M., Araña, J., Espinós, J. P., Ortega-Méndez, J. A., and Doña-Rodríguez, J. M. Effect of TiO₂-Pd and TiO₂-Ag on the photocatalytic oxidation of diclofenac, isoproturon and phenol. *Chem. Eng. J.*, 2016, **298**, 82–95.
- Shahri, Z., Allahkaram, S. R., Soltani, R., and Jafari, H. Optimization of plasma electrolyte oxidation process parameters for corrosion resistance of Mg alloy. *J. Magnes. Alloys*. In press, corrected proof available online 12 December 2018.
- Lin, G-W., Chen, J-S., Tseng, W., and Lu, F-H. Formation of anatase TiO₂ coatings by plasma electrolytic oxidation for photocatalytic applications. *Surf. Coat. Technol.*, 2019, **357**, 28–35.
- Tarkhanova, I. G., Bryzhin, A. A., Gantman, M. G., Yarovaya, T. P., Lukiyanchuk, I. V., Nedozorov, P. M., and Rudnev, V. S. Ce-, Zr-containing oxide layers formed by plasma electrolytic oxidation on titanium as catalysts for oxidative desulfurization. *Surf. Coat. Technol.*, 2019, **362**, 132–140.
- Arrabal, R., Mohedano, M., Matykina, E., Pardo, A., Mingo, B., and Merino, M. C. Characterization and wear behaviour of PEO coatings on 6082-T6 aluminium alloy with incorporated α -Al₂O₃ particles. *Surf. Coat. Technol.*, 2015, **269**, 64–73.
- Drunka, R., Grabis, J., Jankovica, D., Krumina, A., and Rasmane, D. Microwave-assisted synthesis and photocatalytic properties of sulphur and platinum modified TiO₂ nanofibers. *IOP Conf. Ser. Mater. Sci. Eng.*, 2015, **77**, 012010.
- Park, T-E., Choe, H-C., and Brantley, W. A. Bioactivity evaluation of porous TiO₂ surface formed on titanium in mixed electrolyte by spark anodization. *Surf. Coat. Technol.*, 2013, **235**, 706–713.
- Tang, Y., Fu, S., Zhao, K., Xie, G., and Teng, L. Synthesis of TiO₂ nanofibers with adjustable anatase/rutile ratio from Ti sol and rutile nanoparticles for the degradation of pollutants in wastewater. *Ceram. Int.*, 2015, **41**, 13285–13293.
- Cheng, X., Deng, X., Wang, P., and Liu, H. Coupling TiO₂ nanotubes photoelectrode with Pd nano-particles and reduced graphene oxide for enhanced photocatalytic decomposition of diclofenac and mechanism insights. *Sep. Purif. Technol.*, 2015, **154**, 51–59.
- K., Alamelu, B. M., and Jaffar, A. TiO₂-Pt composite photocatalyst for photodegradation and chemical reduction of recalcitrant organic pollutants. *J. Environ. Chem. Eng.*, 2018, **6**, 5720–5731.
- Ramacharyulu, P. V. R. K., Praveen Kumar, J., Prasad, G. K., and Sreedhar, B. Sulphur doped nano TiO₂: synthesis, characterization and photocatalytic degradation of a toxic chemical in presence of sunlight. *Mater. Chem. Phys.*, 2014, **148**, 692–698.
- Sanzone, G., Zimbone, M., Cacciato, G., Ruffino, F., Carles, R., Privitera, V., and Grimaldi, M. G. Ag/TiO₂ nanocomposite for visible light-driven photocatalysis. *Superlattices Microstruct.*, 2018, **123**, 394–402.
- Wang, Y., Jiang, X., and Pan, C. “In situ” preparation of a TiO₂/Eu₂O₃ composite film upon Ti alloy substrate by micro-arc oxidation and its photo-catalytic property. *J. Alloys Compd.*, 2012, **538**, 16–20.
- Yang, J. and Mou, C-Y. Ordered mesoporous Au/TiO₂ nanospheres for solvent-free visible-light-driven plasmonic oxidative coupling reactions of amines. *Appl. Catal. B Environ.*, 2018, **231**, 283–291.
- Yang, J., Zhang, X., Liu, H., Wang, C., Liu, S., Sun, P., et al. Heterostructured TiO₂/WO₃ porous microspheres: preparation, characterization and photocatalytic properties. *Catal. Today*, 2013, **201**, 195–202.
- Drunka, R. Synthesis and Properties of Modified TiO₂ Photocatalysts. Summary of doctoral thesis. University of Latvia, 2018.

Mitmesuguste modifikaatoritega modifitseeritud erineva morfoloogiaga TiO₂ nanostruktuuride fotokatalüütilised omadused

Reinis Drunka, Janis Grabis, Dzidra Jankovica, Dzintra-Arija Rasmene ja Aija Krumina

Uuriti TiO₂ nanotorudest pinnete, nanopoorsete pinnete ja nanokiudude eri parameetritel sünteesi, kasutades titaani anodeerimist, mikroplasma-elektrolüütilist oksüdatsiooni ning mikrolaineaktiveeritud hüdrotermilist sünteesi. Nanostruktuuride saamiseks määrati eri meetodite optimaalsed tingimused. Saadud TiO₂ nanokiude, nanotorusid ja nanopoorseid pindeid modifitseeriti Au, Ag, Pt, Pd, S, WO₃ ja Eu₂O₃ nanoosakestega, parandamaks fotokatalüütilist aktiivsust ultraviolet- ning nähtava valgusega kiiritamisel. Fotokatalüsaatorite fotokatalüütilisi omadusi uuriti metüleeni sinise lahuse lagundamisega ultraviolet- ja nähtava valgusega kiiritamise toimet. Puhtast nanostruktuursest TiO₂-st katalüsaatoriga võrreldes näitasid saadud modifitseeritud fotokatalüsaatorid kõrgemat fotokatalüütilist aktiivsust. Eri meetoditega saadi võrreldavate omadustega modifitseeritud fotokatalüsaatorid.